coatings

MDPI

Article

Perspectives of the Friction Mechanism of Hydrogenated Diamond-Like Carbon Film in Air by Varying Sliding Velocity

Yunhai Liu [1], Bin Zhang [2], Lei Chen [1,3,*], Zhongyue Cao [2], Pengfei Shi [1], Jinwei Liu [1], Junyan Zhang [2] and Linmao Qian [1]

1 Tribology Research Institute, State Key Laboratory of Traction Power, Southwest Jiaotong University, Chengdu 610031, China; liuyun@my.swjtu.edu.cn (Y.L.); pengfei_s@my.swjtu.edu.cn (P.S.); robeant@my.swjtu.edu.cn (J.L.); linmao@swjtu.edu.cn (L.Q.)

2 State Key Laboratory of Solid Lubrication, Lanzhou Institute of Chemical Physics, Chinese Academy of Sciences, Lanzhou 730000, China; bzhang@licp.cas.cn (B.Z.); caozhongyue10@mails.ucas.ac.cn (Z.C.); zhangjunyan@licp.cas.cn (J.Z.)

3 National United Engineering Laboratory for Advanced Bearing Tribology, Henan University of Science and Technology, Luoyang 471023, Henan, China

* Correspondence: chenlei@swjtu.edu.cn; Tel.: +86-28-87634115

Received: 10 August 2018; Accepted: 19 September 2018; Published: 21 September 2018

Abstract: The purpose of the present work is to probe the friction mechanism of hydrogenated diamond-like carbon (H-DLC) film in air by varying sliding velocity (25–1000 mm/s). Friction tests of Al_2O_3 ball against H-DLC film were conducted with a rotational ball-on-disk tribometer. As the sliding velocity increases, both the friction coefficient and the surface wear of H-DLC film decrease, reach the minimum values, and then increase in the high sliding velocity region. Based on the observed results, three main friction mechanisms of H-DLC film—namely graphitization mechanism, transfer layer mechanism, and passivation mechanism—are discussed. Raman analysis indicates that the graphitization of worn surface on the H-DLC film has a negligible contribution to the variation of the friction coefficient and the surface wear. The origin of the sliding velocity dependence is due to the synergistic interaction between the graphitized transfer layer formation and the surface passivation. The present study will not only enrich the understanding of friction mechanism of H-DLC films in air, but will also help to promote their practical engineering applications.

Keywords: diamond-like carbon film; friction mechanism; transfer layer; surface passivation; sliding velocity

1. Introduction

Over the past few decades, energy and material losses caused by friction and wear in machine elements have given rise to the huge economic and environmental burdens for all countries [1]. Therefore, lots of low-friction materials, coatings, and lubricants have been prepared and discovered to regulate the process of friction and wear in machine elements [2,3]. Among the various materials, diamond-like carbon (DLC) film is considered to be one of the most promising solid lubrication materials for industry applications owing to its outstanding physical, chemical, tribological, and optical properties [4–7].

Previously, lots of experimental studies on the tribological properties of DLC films have been carried out by investigating the effects of intrinsic properties, i.e., hydrogen concentration, hardness, metal/nonmetal doping, and so on [8–11]. However, the tribological properties of DLC films depend on not only the intrinsic parameters, but also many extrinsic factors, such as sliding velocity, normal

load, environment atmosphere, and properties of friction interfaces [12–15]. In particular, the effect of sliding velocity on the friction characteristics of DLC films has been extensively studied, giving rise to a large amount of diverging findings [15–17]. For instance, it is noted that the friction coefficient of the DLC films increased from 0.07 to 0.22 with increasing of sliding velocity in air, and the reason is due to the entrapment of more debris particles at the sliding interface [18]. Subsequently, some studies reported that the friction coefficient of H-DLC film decreased from 0.13 to 0.007 with the increase of sliding velocity, and the reason was attributed either to the removal of adsorbed water layer or the increase of the graphitization degree at the sliding interface [19,20]. However, recent study shows that the friction coefficient increases though with a high graphitization degree of the worn surface, where gas passivation is found to play a significant role and the high friction coefficient is mainly due to the insufficient gas passivation [21]. Based on the above research, the effects of sliding velocity on the friction and wear characteristics of DLC films are still not well understood.

The purpose of the present work is to deeply probe the friction mechanism of H-DLC film by varying sliding velocity. In air, the sliding velocity in a broad range from 25 to 1000 mm/s shows a strong effect on the friction behavior of H-DLC film. More surprisingly, the friction coefficient decreases to a minimum value, and then increases as sliding velocity increases. Analysis indicates that the reason is not due to the graphitization of the worn surface on the H-DLC film, but attributed to the synergistic interaction between transfer layer formation and surface passivation. Insights gained from this study are helpful to enrich the understanding of the friction mechanism of H-DLC film in air, as well as promote their practical applications.

2. Materials and Methods

2.1. Preparation of H-DLC Film

In this study, a plasma enhanced chemical-vapor deposition (PECVD) method is used to produce H-DLC films on Si (100) substrates. The deposition processes can be described as the following steps. First, the silicon wafers are ultrasonically cleaned with acetone and ethanol for 30 min and dried in a dry chamber. Then, the cleaned wafers are placed into the vacuum chamber (~10^{-4} Pa) and etched by Ar^+ ions at a pressure of 5 Pa for 30 min. This treatment can not only remove the native oxide and surface contamination but also improve the bonding strength between substrate and deposited material. Besides, to optimize adhesion strength between the film and the silicon substrate, a ~55-nm-thick nitrogen-doped H-DLC film as a buffer layer is firstly grown on the silicon wafer in working atmosphere of a mixture of methane and nitrogen. Finally, the H-DLC film (H% < 20%) is deposited as the outermost layer in the mixed gases of methane and hydrogen [22]. As shown in Figure 1a, thickness of the H-DLC film is characterized as ~866 nm by scanning electron microscopy (SEM, JSM-6701F, JEOL, Tokyo, Japan), and its surface root-mean-square (RMS) roughness is characterized as ~0.20 ± 0.02 nm (averaged at 6 different locations) in scan area of 1 μm × 1 μm by atomic force microscopy (AFM, E-sweep, Hitachi, Tokyo, Japan). Using nanoindentor (Hysitron, TI 750, Minneapolis, MN, USA) with a diamond conical tip (radius = ~2 μm), the load—displacement curve is measured at a maximum indentation depth of 80 nm (Figure 1b). According to the Oliver-Pharr model, hardness and elasticity modulus of the H-DLC film are estimated as ~12.55 and ~102.82 GPa, respectively. Bonding structure of the H-DLC film is analyzed using Raman spectroscopy (JY-HR-800, Jobin Yvon Company, Lille, France), and the Raman spectrum exhibits two main features, a G peak centered at around 1580 cm^{-1} and a D peak at around 1350 cm^{-1}, which is a typical DLC film with an intensity ratio (I_D/I_G) of ~0.41 (Figure 1c) [23].

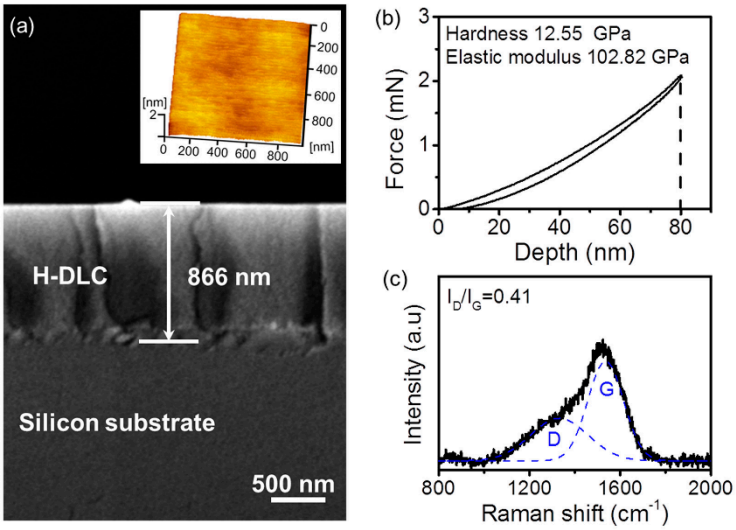

Figure 1. Properties of the hydrogenated diamond-like carbon (H-DLC) film used in the velocity-dependent friction tests. (**a**) SEM image of a fractured cross-section of the H-DLC film. Inset shows the AFM image of the H-DLC film with a RMS roughness of ~0.20 ± 0.02 nm. (**b**) Nanoindentation load−displacement curve of the H-DLC film. (**c**) Raman spectra of the H-DLC film.

2.2. Test Methods

Sliding friction and wear tests for the H-DLC film in air were conducted using a rotational ball-on-disk tribometer (CSM tribometer, CSM Instruments, Peseux, Switzerland) with Al_2O_3 balls (radius R = ~1.5 mm). Before each test, H-DLC film and Al_2O_3 ball were cleaned ultrasonically in ethanol (C_2H_5OH) for ~5 min to eliminate the possible contamination. During the sliding process, the tapplied normal load was maintained at 2 N and the sliding velocity changed from 25 to 1000 mm/s. At the given load, the maximum Hertz contact pressure is calculated as 1042 MPa. Each friction test was conducted at least three times under the same experimental conditions. The relative humidity of the room air is around ~25%. After the sliding tests, all topographies of the worn regions on the H-DLC films formed at various sliding velocities were characterized by three dimensional (3D) profilometry (Superview W1, Chotest Technology Inc., Shenzhen, China), and the corresponding worn surfaces of the Al_2O_3 balls were measured by optical microscope. Bonding structures of the worn surfaces on the H-DLC films and the transfer layer covered on the Al_2O_3 ball surfaces were detected by Raman spectroscopy.

3. Result

3.1. Friction Behavior of the H-DLC Film at Various Sliding Velocities

Figure 2a shows the friction coefficient curves of H-DLC film against Al_2O_3 balls under different sliding velocities in air. In general, the friction coefficients decrease dramatically at the initial stage and then maintain steady under all velocity conditions. The average friction coefficients in the steady stage at various sliding velocities are compared in Figure 2b. It is intriguing to note that the friction coefficient of the H-DLC film decreases from 0.13 to 0.085 as the sliding velocity changes from 25 to 400 mm/s, but gradually increases to 0.096 at 600 mm/s. When the sliding velocity further increases to 1000 mm/s, the friction coefficient of H-DLC film reduces rapidly to 0.05 and increases suddenly to 0.46 after a very short running-in process. The velocity-dependent friction behavior observed in this study is much different from the previously reported results [19,20]. The diverse variation behaviors of the friction coefficient with the sliding velocity imply that the dominant friction mechanism may change at different velocity conditions.

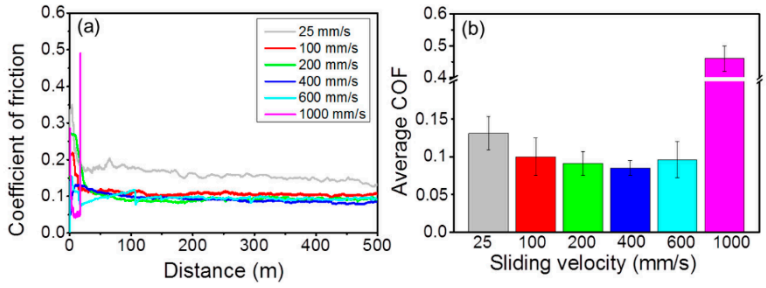

Figure 2. Sliding velocity dependence of friction coefficient on the H-DLC films. (**a**) Friction coefficient curves of the H-DLC film slid against Al_2O_3 balls under the different sliding velocities. (**b**) The average friction coefficient in the steady stage at each condition calculated from (**a**).

3.2. Wear Resistance of the H-DLC Film at Different Sliding Velocities

Figure 3 displays 3D images of the worn tracks on the H-DLC film formed at various sliding velocities after the same sliding distance of 500 m (except that at 1000 mm/s with a distance of ~20 m). Obvious surface wear occurs under all velocity conditions, and especially a much more serious surface damage with a deeper and wider groove is formed at 1000 mm/s. Figure 4 compares the wear depth estimated from the wear tracks shown in Figure 3. With the increase of sliding velocity, the wear depth decreases gradually from ~75 nm at 25 mm/s to ~55 nm at 400 mm/s, and after that, rises to ~76 nm at 600 mm/s and sharply increases to more than 900 nm at 1000 mm/s. Although the sliding distance at 1000 mm/s is twenty five times less than those at other conditions, the wear depth is ten times larger. This value exceeds the thickness of H-DLC film (~866 nm, Figure 1a), indicating the failure of the H-DLC film in a very short distance when the sliding velocity is up to 1000 mm/s. In other words, the high friction coefficient after film failure (Figure 2) may originate from the direct sliding contact between the Al_2O_3 ball and the silicon substrate.

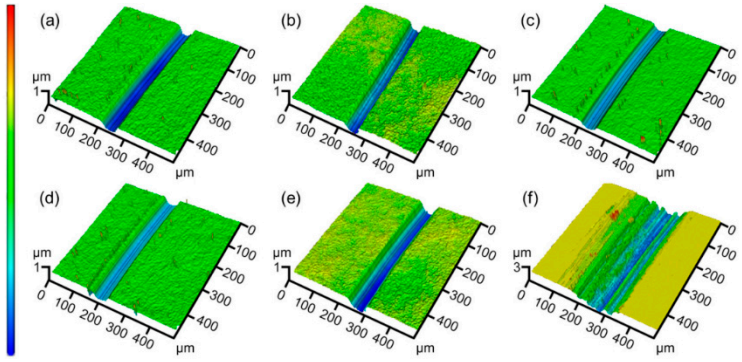

Figure 3. 3D images of the wear tracks formed on the H-DLC films under different sliding velocities. (**a**) 25, (**b**) 100, (**c**) 200, (**d**) 400, (**e**) 600, and (**f**) 1000 mm/s. Note the depth-scale for condition of 1000 mm/s in (**f**) is three times larger than those for other conditions.

The variation of wear resistance shown in Figure 4 is consistent with the velocity-dependent friction behavior of the H-DLC/Al_2O_3 sliding pairs in air (Figure 2). It means that, similar to other sliding interfaces [24–26], the wear of H-DLC film is proportional to the dissipative energy imposed in the friction system. Furthermore, the uniform velocity dependence also indicates that the friction and wear resistance of H-DLC film influenced by sliding velocity may be attributed to the same tribological mechanisms. Previously, three main friction mechanisms of DLC films have been widely recognized, including graphitization mechanism (i.e., graphitization of the DLC material beneath worn surface) [27–29], transfer layer mechanism (i.e., formation of a graphitized transfer layer at the sliding interface) [30–32], and passivation mechanism (i.e., saturation of dangling bonds of carbon atoms at the sliding interface with passivating species) [6,21,33]. Nonmonotonic variation of the friction

and surface wear with the sliding velocity (Figures 2 and 4) implies that one of the above-mentioned mechanisms alone cannot explain the observed phenomenon.

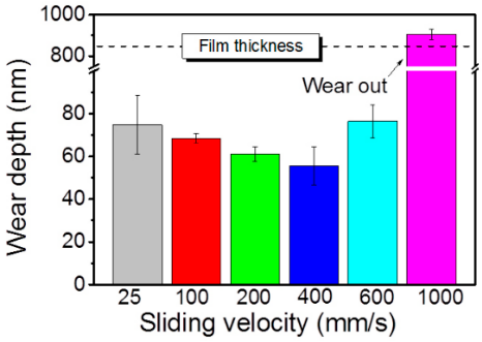

Figure 4. Wear depth of the wear tracks formed on the DLC film under different sliding velocities. The value of the film thickness (~866 nm) is marked by a black dotted line.

4. Discussion

4.1. Role of Graphitization of DLC Material beneath the Worn Surface in the Velocity-Dependence

Previous studies [27,28] reported that the H-DLC material beneath worn surface could be graphitized under shear and compression stresses, and the higher graphitization degree resulted in a lower friction coefficient. Moreover, higher sliding velocity induced the increase of contact frequency and flash temperature, which facilitated the release of hydrogen (H) atoms from the sp^3 structure of H-DLC film, and then shearing of the weakened H depleted layer enhanced the graphitization degree [1,34]. In order to detect the role of graphitization in the velocity-dependent friction and wear behaviors, Raman analyses are performed in the worn regions of H-DLC film after slid against Al_2O_3 balls at different conditions. A typical Raman spectrum of DLC film consists of G and D peaks, where the D peak is due to the breathing modes of sp^2 bonded atoms in the carbon rings, and the G peak is due to the in-plane bond stretching of all pairs of sp^2 bonded atoms in both rings and chains [23,35,36]. The relative intensity ratio of these two peaks (I_D/I_G) can be used to characterize the graphitization degree. Normally, larger value of I_D/I_G corresponds to a higher graphitization degree [37].

Figure 5 compares the Raman spectra measured on the worn surfaces of H-DLC films. To compare the possible structure change of the DLC films after slid at different velocities, the characterized region at 1000 mm/s is chosen at the edge of the wear track where the DLC film is not worn out (i.e., the wear depth is less than the thickness of H-DLC film). The characterized wear tracks are shown in Figure 3. Compared to I_D/I_G of ~0.41 characterized on the original H-DLC film (Figure 1c), no significant change is observed for the values obtained on the worn surfaces of H-DLC films along with the increase of sliding velocity from 25 to 600 mm/s although the friction coefficients in the stable stage are diverse (Figure 2a). Differently, I_D/I_G at 1000 mm/s increases to ~0.71. The highly final friction (Figure 2) and low wear resistance (Figure 4) imply that this high value may mainly originate from the formation of wear debris. Based on the above results, the graphitization of material beneath the worn surfaces of H-DLC films is negligible under those given experimental conditions, and that should have a very limited contribution to the variation of friction with sliding velocity and sliding distance.

4.2. Role of Graphitized Transfer Layer in the Velocity-Dependence

Possible transfer layers formed on the Al_2O_3 counterfaces are checked using optical microscope and Raman spectroscopy. As shown in Figure 6, transfer materials with dark color are visible around the contact regions on the Al_2O_3 ball surfaces after sliding at the velocities of 25–600 mm/s, but is absent at 1000 mm/s. Figure 7 shows the Raman spectra measured on the worn surfaces of the Al_2O_3 balls at various sliding velocities. The D and G peaks can be detected when the velocity is less than 600 mm/s, supporting the formation of transfer layer. The Raman spectrum of the transfer layer at

25 mm/s shows main signal of amorphous carbon structure [23,35,36]. Furthermore, the center of G peak at 600 mm/s is found to shift a larger amplitude compared to other conditions, namely from 1580 to 1593 cm^{-1}. It indicates that more graphite-like structure may form during sliding process at higher velocity [23,35,36]. However, no marked signal is observed at 1000 mm/s (Figure 7f) that confirms no transfer layer existing on the Al_2O_3 counterface under this condition.

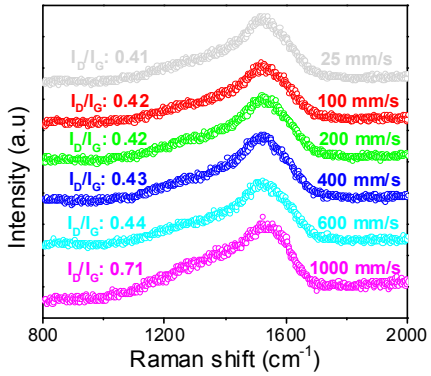

Figure 5. Raman spectra measured on the worn surfaces of the H-DLC films at different sliding velocities.

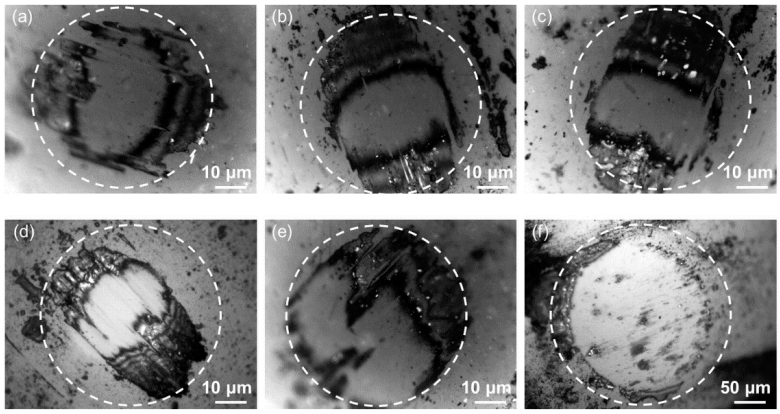

Figure 6. Optical micrographs of the worn surfaces on the Al_2O_3 balls after sliding against the H-DLC film at various sliding velocities. (**a**) 25, (**b**) 100, (**c**) 200, (**d**) 400, (**e**) 600, and (**f**) 1000 mm/s. Note that the scale at 1000 mm/s in (**f**) is five times larger than that at other conditions.

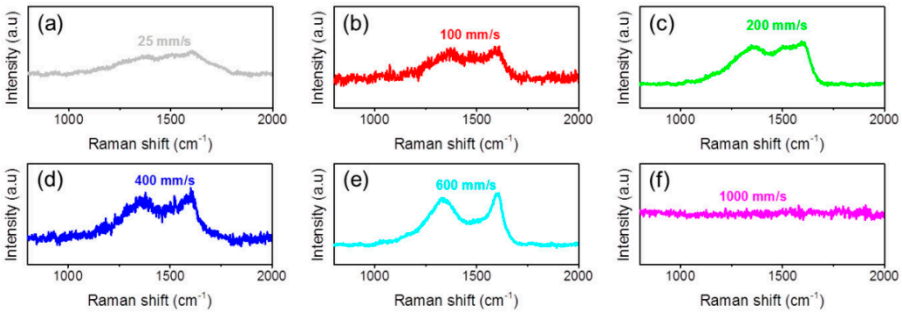

Figure 7. Raman spectra of the worn surfaces on Al_2O_3 sliding against H-DLC under different sliding velocities. (**a**) 25, (**b**) 100, (**c**) 200, (**d**) 400, (**e**) 600, and (**f**) 1000 mm/s.

Although the nonuniform coverage of the transfer layer on the counterfaces may lead to the increase in dispersion, the significantly larger degree of transfer layer formation can be observed at higher sliding velocity in the range of 25–600 mm/s (Figure 7a–e). These results mean that the portion of

low shear resistance region covered by the highly graphitized transfer layer increases with the increase of sliding velocity [19,31]. Moreover, the removal of transfer layer at 1000 mm/s may be the main reason for the increase of friction coefficient, which is found in our previous study [22]. It is consistent with the velocity-dependent friction behavior that the degree of transfer layer formation corresponds to a lower friction coefficient (Figure 2). Therefore, the good agreement between the friction coefficient and the degree of transfer layer formation reveals that the formation of the graphitized transfer layer has a strong contribution to the low friction coefficient of the H-DLC films after the initial running-in process.

As described above, the reason of low friction coefficient is not the graphitization of the worn surface on the H-DLC film, but the formation of the graphitized transfer layer. However, this mechanism can not explain the increase of friction coefficient though the degree of transfer layer formation at 600 mm/s is larger compared to other cases. It implies that another friction mechanism (such as passivation mechanism) may play an important role in the variation of friction coefficient on the H-DLC film in air.

4.3. Role of Surface Passivation in the Velocity-Dependence

According to the passivation mechanism [6,21,33], saturation of the dangling carbon bonds on the sliding interface with passivating species may result in a low friction coefficient. In the present study, the water molecules, nitrogen and other gases in air may influence the friction behavior of H-DLC film. When the sliding velocity raises to more than 600 mm/s, it will enlarge the rotating frequency and short the time of friction heat diffusion. Then, the larger degree of friction-induced temperature rise may lead to the decrease of gas adsorption, resulting in the insufficient passivation of dangling bonds of carbon atoms during the sliding process [21,38,39].

To detect possible effect of the surface passivation on the velocity dependence of friction and wear resistance, two friction tests with only the change of rotating frequency are carried out. The two rotational radii include 3 mm and 8 mm (inset schematic in Figure 8). The sliding velocity keeps 50 mm/s. Then, the rotating frequencies can be controlled to be ~2.65 and ~1 s^{-1}, respectively. As shown in Figure 8, significant difference of the friction coefficient in the stable stage is observed at the sliding distance above ~100 m. The close values in the initial 100 m distance may be due to the adequate surface passivation because of the small contact area in the early sliding phase. Physically, larger rotating frequency can promote growth of flash temperature [38]. The higher friction coefficient at ~2.65 s^{-1} (3 mm radius) than that at ~1 s^{-1} (8 mm radius) indicates that the contribution of temperature rise induced graphitization on the friction difference can be rule out. Then, the increase of friction force at a larger rotating frequency is overwhelmingly likely the insufficient surface passivation [21,39]. Similarly, high sliding velocity at a constant rotating radius corresponds to a large rotating frequency. Therefore, the insufficient passivation may be the reason for the rise of friction coefficient on the H-DLC film when the sliding velocity increases to 600 mm/s (Figure 2b).

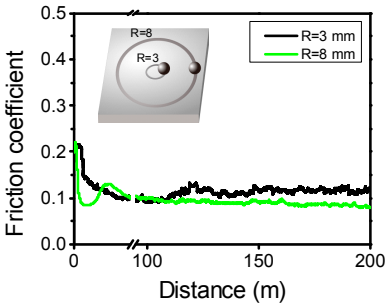

Figure 8. The friction coefficients of the H-DLC/Al_2O_3 sliding pairs under different rotational radii. The inset shows the experimental sketch under different rotational radii.

In summary, both the graphitized transfer layer and the surface passivation should significantly contribute to the nonmonotonous variation of the velocity-dependent friction of the H-DLC film against Al_2O_3 balls in air. With the increase of sliding velocity, the graphitized transfer layer formed during the sliding process can lower the friction, conversely, the insufficient surface passivation enlarges the friction coefficient. The transformation of the velocity-dependent friction shown in Figure 2 indicates that these two contributions may be balanced at a certain sliding velocity, below which the transfer layer mechanism dominates the friction behavior, and above which the passivation mechanism plays a more important role. However, the transfer layer cannot be held on the sliding interface when the sliding velocity is too large, then the H-DLC film is worn out rapidly (such as 1000 mm/s).

5. Conclusions

The friction and wear mechanisms of the H-DLC film against Al_2O_3 balls in air are investigated by varying sliding velocity. The main conclusions can be drawn as below.

- The friction coefficient and wear resistance of the H-DLC film strongly depend on the sliding velocity. With the increase of sliding velocity, both the friction coefficient and wear resistance decrease gradually below 400 mm/s and then increase above this critical velocity.
- No significant change of bonding structure is observed on the worn surface of H-DLC film at various sliding velocities that eliminates the graphitization of H-DLC material beneath the worn region contributing to the variation of friction coefficient.
- Both the transfer layer and surface passivation mechanism contribute to the velocity dependence of friction coefficient and wear resistance on the H-DLC film in air. The transfer layer mechanism may dominate the friction behavior at a relatively low sliding velocity, while the passivation mechanism may play a more important role at high sliding velocity.

Author Contributions: Conceptualization, Y.L., Z.C., P.S. and J.L.; Data Curation, Y.L.; Formal Analysis, Y.L., L.C., B.Z., Z.C., P.S. and J.L.; Funding Acquisition, L.Q.; Investigation, Y.L. and Z.C.; Methodology, Y.L.; Resources, B.Z., Z.C. and J.Z.; Supervision, J.Z. and L.Q.; Writing-Original Draft Preparation, Y.L.; Writing-Review & Editing, Y.L., L.C. and B.Z.

Funding: The authors are grateful for the financial support from the National Natural Science Foundation of China (51505391, 51875486 and 51527901), Self-developed Project of State Key Laboratory of Traction Power (2017TPL_Z02) and the Fundamental Research Funds for the Central Universities (2682016CX026).

Acknowledgments: The authors thank Ningning Zhou at Beijing Institute of Control Engineering for his technical supports and materials used for experiments.

Conflicts of Interest: The authors declare no conflict of interest.

References

1. Erdemir, A.; Eryilmaz, O. Achieving superlubricity in DLC films by controlling bulk, surface, and tribochemistry. *Friction* **2014**, *2*, 140–155. [CrossRef]
2. Zahid, R.; Masjuki, H.H.; Varman, M.; Kalam, M.A.; Mufti, R.A.; Mohd Zulkifli, N.W.B.; Gulzar, M.; Nor Azman, S.S.B. Influence of intrinsic and extrinsic conditions on the tribological characteristics of diamond-like carbon coatings: A review. *J. Mater. Res.* **2016**, *31*, 1814–1836. [CrossRef]
3. Zhang, P.; He, H.; Chen, C.; Xiao, C.; Chen, L.; Qian, L. Effect of abrasive particle size on tribochemical wear of monocrystalline silicon. *Tribol. Int.* **2017**, *109*, 222–228. [CrossRef]
4. Muguruma, T.; Iijima, M.; Kawaguchi, M.; Mizoguchi, I. Effects of sp^2/sp^3 ratio and hydrogen content on in vitro bending and frictional performance of DLC-coated orthodontic stainless steels. *Coatings* **2018**, *8*, 199. [CrossRef]
5. Shi, W.L.; Wei, X.T.; Zhang, W.; Wang, Z.G.; Dong, C.H.; Li, S. Developments and applications of diamond-like carbon. *Appl. Mech. Mater.* **2017**, *864*, 14–24. [CrossRef]
6. Cui, L.; Lu, Z.; Wang, L. Toward low friction in high vacuum for hydrogenated diamondlike carbon by tailoring sliding interface. *ACS Appl. Mater. Interfaces* **2013**, *5*, 5889–5893. [CrossRef] [PubMed]

7. Erdemir, A.; Ramirez, G.; Eryilmaz, O.L.; Narayanan, B.; Liao, Y.; Kamath, G.; Sankaranarayanan, S.K. Carbon-based tribofilms from lubricating oils. *Nature* **2016**, *536*, 67–71. [CrossRef] [PubMed]
8. Wang, F.; Wang, L.; Xue, Q. Fluorine and sulfur co-doped amorphous carbon films to achieve ultra-low friction under high vacuum. *Carbon* **2016**, *96*, 411–420. [CrossRef]
9. Cao, Z.; Zhao, W.; Liu, Q.; Liang, A.; Zhang, J. Super-elasticity and ultralow friction of hydrogenated fullerene-like carbon films: Associated with the size of graphene sheets. *Adv. Mater. Interfaces* **2018**, *5*, 1701303. [CrossRef]
10. Berman, D.; Deshmukh, S.A.; Sankaranarayanan, S.K.; Erdemir, A.; Sumant, A.V. Macroscale superlubricity enabled by graphene nanoscroll formation. *Science* **2015**, *348*, 1118–1122. [CrossRef] [PubMed]
11. Bhowmick, S.; Banerji, A.; Lukitsch, M.J.; Alpas, A.T. The high temperature tribological behavior of Si, O containing hydrogenated diamond-like carbon (a-C:H/a-Si:O) coating against an aluminum alloy. *Wear* **2015**, *330*, 261–271. [CrossRef]
12. Kano, M. Overview of DLC-coated engine components. In *Coating Technology for Vehicle Applications*, 1st ed.; Cha, S.C., Erdemir, A., Eds.; Springer: Cham, Switzerland, 2015; pp. 37–62.
13. Chen, Z.; Ren, X.; Ren, L.; Wang, T.; Qi, X.; Yang, Y. Improving the tribological properties of spark-anodized titanium by magnetron sputtered diamond-like carbon. *Coatings* **2018**, *8*, 83. [CrossRef]
14. Shi, J.; Gong, Z.; Wang, C.; Zhang, B.; Zhang, J. Tribological properties of hydrogenated amorphous carbon films in different atmospheres. *Diam. Relat. Mater.* **2017**, *77*, 84–91. [CrossRef]
15. Kim, D.-W.; Kim, K.-W. Effects of sliding velocity and ambient temperature on the friction and wear of a boundary-lubricated, multi-layered DLC coating. *Wear* **2014**, *315*, 95–102. [CrossRef]
16. Solis, J.; Zhao, H.; Wang, C.; Verduzco, J.A.; Bueno, A.S.; Neville, A. Tribological performance of an H-DLC coating prepared by PECVD. *Appl. Surf. Sci.* **2016**, *383*, 222–232. [CrossRef]
17. Ciniero, A.; Le Rouzic, J.; Reddyhoff, T. The use of triboemission imaging and charge measurements to study DLC coating failure. *Coatings* **2017**, *7*, 129. [CrossRef]
18. Li, K.; Zhou, Z.; Bello, I.; Lee, C.S.; Lee, S.T. Study of tribological performance of ECR–CVD diamond-like carbon coatings on steel substrates. *Wear* **2005**, *258*, 1577–1588. [CrossRef]
19. Kim, D.W.; Kim, K.W. Effects of sliding velocity and normal load on friction and wear characteristics of multi-layered diamond-like carbon (DLC) coating prepared by reactive sputtering. *Wear* **2013**, *297*, 722–730. [CrossRef]
20. Kim, H.I.; Lince, J.R.; Eryilmaz, O.L.; Erdemir, A. Environmental effects on the friction of hydrogenated DLC films. *Tribol. Lett.* **2006**, *21*, 51–56. [CrossRef]
21. Cui, L.; Lu, Z.; Wang, L. Probing the low-friction mechanism of diamond-like carbon by varying of sliding velocity and vacuum pressure. *Carbon* **2014**, *66*, 259–266. [CrossRef]
22. Liu, Y.; Yu, B.; Cao, Z.; Shi, P.; Zhou, N.; Zhang, B.; Zhang, J.; Qian, L. Probing superlubricity stability of hydrogenated diamond-like carbon film by varying sliding velocity. *Appl. Surf. Sci.* **2018**, *439*, 976–982. [CrossRef]
23. He, M.; Yeo, C. Evaluation of thermal degradation of DLC Film using a novel Raman spectroscopy technique. *Coatings* **2018**, *8*, 143. [CrossRef]
24. Chen, L.; He, H.; Wang, X.; Kim, S.H.; Qian, L. Tribology of Si/SiO_2 in humid air: Transition from severe chemical wear to wearless behavior at nanoscale. *Langmuir* **2015**, *31*, 149–156. [CrossRef] [PubMed]
25. Aghdam, A.B.; Khonsari, M.M. Prediction of wear in reciprocating dry sliding via dissipated energy and temperature rise. *Tribol. Lett.* **2013**, *50*, 365–378. [CrossRef]
26. Zhang, P.; Chen, C.; Xiao, C.; Chen, L.; Qian, L. Comparison of wear methods at nanoscale: Line scanning and area scanning. *Wear* **2018**, *400*, 137–143. [CrossRef]
27. Liu, Y.; Meletis, E.I. Evidence of graphitization of diamond-like carbon films during sliding wear. *J. Mater. Sci.* **1997**, *32*, 3491–3495. [CrossRef]
28. Liu, Y.; Erdemir, A.; Meletis, E.I. An investigation of the relationship between graphitization and frictional behavior of DLC coatings. *Surf. Coat. Technol.* **1996**, *86*, 564–568. [CrossRef]
29. Wang, Y.; Guo, J.; Gao, K.; Zhang, B.; Liang, A.; Zhang, J. Understanding the ultra-low friction behavior of hydrogenated fullerene-like carbon films grown with different flow rates of hydrogen gas. *Carbon* **2014**, *77*, 518–524. [CrossRef]
30. Scharf, T.W.; Singer, I.L. Role of third bodies in friction behavior of diamond-like nanocomposite coatings studied byin situtribometry. *Tribol. Trans.* **2002**, *45*, 363–371. [CrossRef]

31. Manimunda, P.; Al-Azizi, A.; Kim, S.H.; Chromik, R.R. Shear-induced structural changes and origin of ultralow friction of hydrogenated diamond-like carbon (DLC) in dry environment. *ACS Appl. Mater. Interfaces* **2017**, *9*, 16704–16714. [CrossRef] [PubMed]
32. Chen, X.; Kato, T.; Nosaka, M. Origin of superlubricity in a-C:H:Si films: A relation to film bonding structure and environmental molecular characteristic. *ACS Appl. Mater. Interfaces* **2014**, *6*, 13389–13405. [CrossRef] [PubMed]
33. Cui, L.; Lu, Z.; Wang, L. Environmental effect on the load-dependent friction behavior of a diamond-like carbon film. *Tribol. Int.* **2015**, *82*, 195–199. [CrossRef]
34. Al Mahmud, K.A.; Kalam, M.A.; Masjuki, H.H.; Mobarak, H.M.; Zulkifli, N.W. An updated overview of diamond-like carbon coating in tribology. *Crit. Rev. Solid State Mater. Sci.* **2015**, *40*, 90–118. [CrossRef]
35. Casiraghi, C.; Ferrari, A.C.; Robertson, J. Raman spectroscopy of hydrogenated amorphous carbons. *Phys. Rev. B* **2005**, *72*, 085401. [CrossRef]
36. Prawer, S.; Nugent, K.W.; Lifshitz, Y.; Lempert, G.D.; Grossman, E.; Kulik, J.; Avigal, I.; Kalish, R. Systematic variation of the Raman spectra of DLC films as a function of sp^2:sp^3 composition. *Diam. Relat. Mater.* **1996**, *5*, 433–438. [CrossRef]
37. Song, H.; Ji, L.; Li, H.; Liu, X.; Zhou, H.; Wang, W.; Chen, J. Perspectives of friction mechanism of a-C:H film in vacuum concerning the onion-like carbon transformation at the sliding interface. *RSC Adv.* **2015**, *5*, 8904–8911. [CrossRef]
38. Byrne, C.; Wang, Z. Influence of thermal properties on friction performance of carbon composites. *Carbon* **2001**, *39*, 1789–1801. [CrossRef]
39. Yen, B.K. An investigation of friction and wear mechanisms of carbon-carbon composites in nitrogen and air at elevated temperatures. *Carbon* **1996**, *34*, 489–498. [CrossRef]